Fundamental Research xxx (xxxx) xxx

Contents lists available at ScienceDirect

Fundamental Research

journal homepage: http://www.keaipublishing.com/en/journals/fundamental-research/

Article

Carbon fluxes and soil carbon dynamics along a gradient of biogeomorphic succession in alpine wetlands of Tibetan Plateau

Hao Wang [a,b,*], Lingfei Yu [c], Litong Chen [d], Zhenhua Zhang [d], Xuefei Li [e], Naishen Liang [f], Changhui Peng [g], Jin-Sheng He [b,h,*]

[a] State Key Laboratory of Herbage Improvement and Grassland Agro-ecosystems, College of Ecology, Lanzhou University, Lanzhou 730000, China
[b] Institute of Ecology, College of Urban and Environmental Sciences, and Key Laboratory for Earth Surface Processes of the Ministry of Education, Peking University, Beijing 100871, China
[c] State Key Laboratory of Vegetation and Environmental Change, Institute of Botany, Chinese Academy of Sciences, Beijing 100093, China
[d] Qinghai Haibei National Field Research Station of Alpine Grassland Ecosystem, and Key Laboratory of Adaptation and Evolution of Plateau Biota, Northwest Institute of Plateau Biology, Chinese Academy of Sciences, Xining 810008, China
[e] Institute for Atmospheric and Earth System Research (INAR)/Physics, Faculty of Science, University of Helsinki, P.O. Box 68, Helsinki FI-00014, Finland
[f] Earth System Division, National Institute for Environmental Studies, Tsukuba, Ibaraki 305-8506, Japan
[g] Department of Biology Sciences, Institute of Environment Sciences, University of Quebec at Montreal, Montreal, QC H3C 3P8, Canada
[h] State Key Laboratory of Herbage Improvement and Grassland Agro-ecosystems, College of Pastoral Agriculture Science and Technology, Lanzhou University, Lanzhou 730000, China

ARTICLE INFO

Article history:
Received 26 June 2022
Received in revised form 16 September 2022
Accepted 19 September 2022
Available online xxx

Keywords:
Carbon dioxide
Methane
Soil organic carbon
Climate change
Hydrological change

ABSTRACT

Hydrological changes under climate warming drive the biogeomorphic succession of wetlands and may trigger substantial carbon loss from the carbon-rich ecosystems. Although many studies have explored the responses of wetland carbon emissions to short-term hydrological change, it remains poorly understood how the carbon cycle evolves with hydrology-driven wetland succession. Here, we used a space-for-time approach across hydrological gradients on the Tibetan Plateau to examine the dynamics of ecosystem carbon fluxes (carbon dioxide (CO_2) and methane (CH_4)) and soil organic carbon pools during alpine wetland succession. We found that the succession from mesic meadow to fen changed the seasonality of both CO_2 and CH_4 fluxes, which was related to the shift in plant community composition, enhanced regulation of soil hydrology and increasing contribution of spring-thaw emission. The paludification caused a switch from net uptake of gaseous carbon to net release on an annual timescale but produced a large accumulation of soil organic carbon. We attempted to attribute the paradox between evidence from the carbon fluxes and pools to the lateral carbon input and the systematic changes of historical climate, given that the wetlands are spatially low-lying with strong temporal climate-carbon cycle interactions. These findings demonstrate a systematic change in the carbon cycle with succession and suggest that biogeomorphic succession and lateral carbon flows are both important for understanding the long-term dynamics of wetland carbon footprints.

1. Introduction

Globally, wetlands store approximately one-third of soil carbon [1] but contribute ~31% of annual methane (CH_4) emissions [2]. Waterlogged conditions and subsequent biogeomorphic succession are key to shaping carbon storage and carbon cycle characteristics in approximately half of global wetlands [3]. In biogeomorphic succession, organisms (e.g., vegetation) engineer landforms to meet their requirements by reciprocal organism-landform interactions [4,5]. Such processes, including concurrent changes in vegetation, microorganisms, hydrology and soil organic matter, regulate the form (carbon dioxide (CO_2) or CH_4) and magnitude of ecosystem carbon emissions [6,7]. Climate change has significantly changed surface hydrology and triggered wetland biogeomorphic succession [8]. For instance, nearly 15% of boreal permafrost peatlands have been lost, but temperate peatlands have slowly increased since 1850 [4]. Although many studies have examined the effect of short-term hydrological changes on carbon emissions [9,10], it remains unclear how the carbon cycle evolves with hydrology-driven wetland biogeomorphic succession.

One typical process of wetland biogeomorphic succession is paludification, driven externally by shifting hydrological balance [11].

* Corresponding authors.
E-mail addresses: wanghao@lzu.edu.cn (H. Wang), jshe@pku.edu.cn (J.-S. He).

https://doi.org/10.1016/j.fmre.2022.09.024

Please cite this article as: H. Wang, L. Yu, L. Chen et al., Carbon fluxes and soil carbon dynamics along a gradient of biogeomorphic succession in alpine wetlands of Tibetan Plateau, Fundamental Research, https://doi.org/10.1016/j.fmre.2022.09.024

Generally, as paludification occurs, reduced soil aeration slows soil organic matter decomposition [12] and influences plant CO_2 fixation by changing photosynthetic physiology and community composition [10,13]. A lower redox potential also provides a favorable environment for soil methanogens and stimulates CH_4 production [9]. However, it remains poorly understood whether the impact of the increased CH_4 emissions on the climate system is canceled out by the impact of the decreased soil CO_2 emissions during paludification when considering that CH_4 has a higher global warming potential (GWP) than CO_2 [14,15]. It is also of great importance to elucidate the change in the temporal dynamics of ecosystem carbon fluxes during paludification when predicting future carbon emissions [6]. The temporal dynamics of carbon fluxes can be influenced by shifts in plant and microbial community composition because the responses of organisms to environmental fluctuations as well as plant phenology often differ among species [6,7]. In addition, it has been documented that soil freeze-thaw processes produce CO_2 and CH_4 emission peaks in high-latitude and high-elevation ecosystems [12,16–18]. Although hydrology regulates soil freeze-thaw characteristics, few studies have examined the effects of paludification on ecosystem carbon emissions during the soil freeze-thaw period.

The Tibetan Plateau, as the world's highest unit and the "Water Tower of Asia", harbors a large amount of soil carbon [19,20]. Over the past five decades, the plateau has experienced climate warming at a rate twice that of the global average [21]. Such rising temperature, on the one hand, increases permanent surface water by 20% and creates new wetlands on the Tibetan Plateau as a result of glacier retreat and permafrost thawing [8,22]; on the other hand, it reduces the water table of some wetlands due to the underlying permafrost thawing [23]. Additionally, ensemble habitat distribution models predict that plateau wetlands will shrink and transition to other ecosystem types in the coming decades if warming continues [24]. Alpine succession may cause significant climate risks associated with the form and magnitude of carbon emissions. In this study, we used a space-for-time approach to examine how ecosystem carbon fluxes evolve during alpine biomorphic succession from precipitation-dominated meadows to groundwater-dominated wetlands (Fig. 1a). We hypothesized that paludification would stimulate net ecosystem CO_2 uptake in addition to increasing CH_4 emissions, given that waterlogged conditions would slow soil organic matter decomposition and reduce CO_2 emissions (Fig. 1b). As a result, we hypothesized that the net effects of paludification would be enhanced soil carbon accumulation but higher GWP driven primarily by the increasing CH_4 emissions.

2. Materials and methods

2.1. Site description

We conducted this study at the Luanhaizi wetland (37°35′ N, 101°20′ E, 3250 m above sea level; Fig. S1a), located approximately 2 km from the Qinghai Haibei National Field Research Station of Alpine Grassland Ecosystem in the northeastern part of the Tibetan Plateau. The area has a continental monsoon climate, with a short, cool summer and a long, cold winter. During our study period from 2010 to 2014, the mean annual air temperature of the study site was −1.3 °C; the mean annual precipitation was 465 mm, with 81% of the precipitation falling from June to October.

The Luanhaizi wetland is mainly occupied by fens, wet meadows are distributed at the margin of fens, and mesic meadows are distributed outside of wet meadows (Fig. S1b). The three alpine ecosystems, representing approximately 30% of the whole Tibetan Plateau (Fig. S1a), together form the typical series of alpine biomorphic succession, as demonstrated by the vertical distribution of plant residues and the similarity of vegetation composition and seed bank [25,26]. They have different soil and hydrological characteristics and are dominated by different perennial plant species. The source of water for fens is primarily groundwater. The fens are permanently flooded in the growing season and are dominated by *Carex pamirensis* (Fig. 1a). The hydrology of wet meadows is mainly controlled by precipitation, and they are intermittently flooded and dominated by *Kobresia tibetica*. In contrast, the mesic meadows have well-drained soils and are dominated by *Stipa aliena* and *Elymus nutans*. Across the growing seasons of 2010–2014, the water table level and the 5-cm soil moisture were −0.16 cm and 61.2% for fens, −27.7 cm and 37.2% for wet meadows, and −428.4 cm and 27.0% for mesic meadows, respectively (Table S1, Fig. S2). In addition, the fens are covered by ice during winter, while the wet meadows and mesic meadows have no persistent thick snowpack [12,27]. More detailed information on the three ecosystems is provided in the Supporting Information (Table S1).

2.2. Experimental design

We conducted this experiment along a transect from mesic meadow to wet meadow and to fen. The transect was 200 m long (north-south) and 50 m wide (east-west) with an elevation gradient of approximately 5 m across its entire length (Fig. S1b). Prior to the experiment, we fenced the transect to remove the potential impacts of grazing. We also built a straight boardwalk to minimize disturbance during sampling.

2.3. Ecosystem carbon flux measurement

Manual static chamber method. For each ecosystem, we deployed five fixed collars (0.4 × 0.4 × 0.1 m) that were 10 m apart for monitoring ecosystem carbon fluxes using the manual static chamber method. Specifically, we used static transparent chambers (0.4 × 0.4 × 0.6 m) combined with an infrared gas analyzer (LI-6400, LI-COR Inc., Lincoln, NE, USA) to measure the net ecosystem CO_2 exchange (NEE) [9]. During the measurement period, we placed a removable transparent chamber on the fixed collar, which was inserted 5 cm into the soil and sealed with water. We then ran a micro fan to mix the gas in the removable chamber. The mixed gas was pumped into an LI-6400. The CO_2 concentrations were measured and recorded at 10-s intervals within 1 min after the LI-6400 reading reached steady state. We calculated the NEE by the slope of the linear regression of the six consecutive CO_2 concentrations over time. When the NEE measurement finished, we ventilated the transparent chamber and repeated the measurement, but the chamber was covered with a black cloth. Thus, the measured flux represented the ecosystem respiration. We calculated the gross ecosystem productivity by subtracting ecosystem respiration from NEE.

We used static opaque chambers (0.4 × 0.4 × 0.4 m) and gas chromatography (Agilent 7890A, Agilent Co., Santa Clara, CA, USA) to measure the ecosystem CH_4 flux [9]. We placed the removable opaque chamber on the fixed collar and collected four gas samples using 100 ml syringes at 10 min intervals. Gas samples were analyzed within 48 h on a gas chromatograph equipped with a flame ionization detector. We calculated the CH_4 flux by the slope of the linear regression between CH_4 concentrations and sampling time.

In this study, we used the manual static chamber method to measure carbon fluxes in mesic meadows from 2011 to 2014 and in wet meadows and fens in the growing seasons of 2010–2013 (Fig. S3). We conducted each measurement between 9:00 and 12:00 local time on sunny days twice a month during growing seasons and once a month during non-growing seasons. We also monitored the daily dynamics of CO_2 and CH_4 fluxes at 2 h intervals in July for calibration of the proportions of daily values to daytime (9:00–12:00) values.

Continuous automated chamber method. We established a multichannel automated chamber system to monitor the NEE and CH_4 fluxes at 1 h resolution at the wet meadow and fen during 2011–2014 (Fig. S3). The automated chamber system consisted of twenty transparent chambers, a multichannel gas sampler, a CR1000 datalogger (Campbell Scientific, Utah, USA) and a CO_2/CH_4/H_2O gas analyzer (G1301,

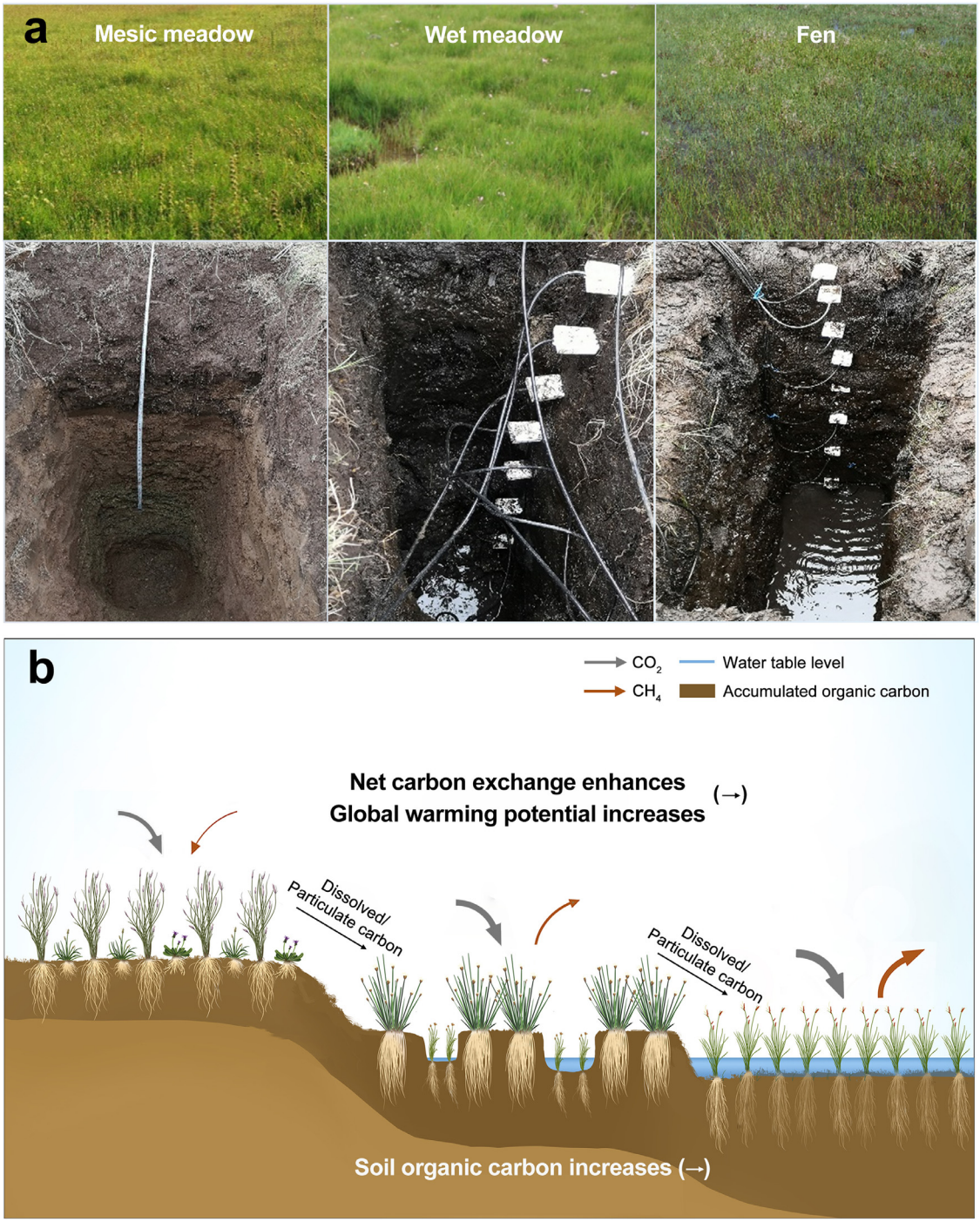

Fig. 1. Characteristics of the studied ecosystems along alpine biogeomorphic succession and the hypothesis in this study. (a) Above- and belowground characteristics; (b) the hypothesis that paludification increases net carbon dioxide (CO_2) uptake due to slowed soil organic matter decomposition and produces higher methane (CH_4) by enhancing anaerobic respiration. As a result, the global warming potential of gaseous carbon exchanges increases and soil organic carbon accumulates.

Picarro, Santa Clara, CA, USA) [12]. We placed the chambers (ten without any treatment and ten with clipping treatment) within an area of 30 m diameter. In this study, we focused on the ten chambers without treatments.

Over the course of an hour, the twenty automated chambers took turns working for 3 min. As a chamber ran, its top lids and side windows closed, and two built-in fans ran. The mixed air was pumped to the Picarro G1301 analyzer to analyze the CO_2 and CH_4 concentrations, and then the analyzed air was returned to the chamber through a circuit. Once the operation was finished, the lids and windows of the chamber remained open, allowing atmospheric turbulence and rainfall. We calculated the hourly ecosystem carbon fluxes by the rates of concentration change during the three minutes of chamber closure.

For better comparability between the automated chamber and static chamber methods, we established linear relationships between their simultaneously measured CO_2 and CH_4 fluxes (Fig. S4). We used the linear relationships to calibrate the daily CO_2 and CH_4 fluxes measured by a manual static chamber.

2.4. Plant and soil sampling

For each ecosystem, we established five plant sampling quadrats (2 × 2 m) that were in parallel with the gaseous carbon flux monitoring plots. In the peak growing seasons of 2012–2014, we harvested, dried, and weighed plant aboveground parts, and the measured biomass was defined as the aboveground net primary productivity. We also separated the harvested biomass into different species to investigate species richness and abundance. In 2014, we measured plant belowground biomass by collecting root samples at depths of 0–100 cm using a 5.0 cm diameter soil auger. Living roots were carefully picked based on their color, consistency and attached fine roots, but we could not separate new roots of the current year from old roots.

We surveyed three soil profiles of 0–180 cm to estimate the soil organic carbon density in each ecosystem using soil pits in 2019. We collected the soil at layers of 0–10 cm, 10–30 cm, 30–50 cm, 50–70 cm, 70–90 cm, 90–120 cm, 120–150 cm and 150–180 cm using a standard container with a diameter of 5 cm and a volume of 100 cm^3 (Fig. S5). One part of the soil samples was used to measure the soil bulk density. The other part of the soil samples was air-dried, sieved, and used to measure the soil organic carbon content by combustion using an elemental analyzer (2400 II CHN Elemental Analyzer, Perkin-Elmer, USA). We calculated the soil organic carbon density (SOCD, kg C m^{-2}) using the following equation:

$$SOCD = 0.01 \times SOCC \times BD \times Depth$$

where SOCC is the soil organic carbon content (g kg^{-1}), BD is the soil bulk density (g cm^{-3}) and Depth is the soil layer (cm). Although the soil organic carbon measurement was taken several years later than the gaseous carbon flux monitoring, the soil carbon density should not significantly change between the two study periods because our studied ecosystems stored large amounts of soil organic carbon and had a low soil carbon decomposition rate [12,20].

2.5. Meteorological measurements

We collected meteorological information using a weather station within our study plot. Air temperature and relative humidity were measured with an HMP45C Vaisala temperature and relative humidity probe (HMP45C, Vaisala Inc., Woburn, MA, USA), precipitation was recorded with a tipping-bucket rain gage (TE525MM, Texas Electronics, Dallas, Texas, USA), and photosynthetic active radiation was measured using a quantum sensor (LI-190SB; Li-Cor, Lincoln, Nebraska, USA). In addition, we measured soil temperature and moisture using EM 50 sensors (Decagon Devices Inc., USA). We monitored the water table depth in the wet meadow using slotted polyvinyl chloride pipes and in the fen using HOBO dataloggers (Onset Computer, Bourne, MA, USA).

2.6. Data analysis

We used a back-propagation artificial neural network (ANN) approach to gap-fill the hourly and daily carbon flux data (the "*newff*" function; R "AMORE" package, version 0.2–16) [17,28]. The ANN is a machine learning algorithm and has a generalization capability beyond the training data by learning from examples [29]. Specifically, we first determined an array of input variables and neurons in our ANN analysis based on the rule of parsimony and good gap-filling performance. The input variables included air temperature, relative humidity, photosynthetic active radiation, soil temperature, soil volumetric water content and the fuzzy sets which represented the time of day and the season of year [29]. Then, we ran the ANN 500 times for the raw data of each plot [17]. In each run, we sampled 70% of the raw data as the training dataset to establish the network and used the remaining 30% of the raw data as the test dataset to assess its performance. A lower value of the root mean square error represents a higher fitting accuracy of the network. Finally, we filtered the 25 best runs that had the lowest root mean square error values and used their averages to gap-fill the flux data [17].

We performed piecewise structural equation modeling to investigate the relative importance of photosynthetic active radiation, water table depth, soil temperature and soil moisture in regulating gaseous carbon fluxes during the growing season (the "*psem*" function; R "piecewiseSEM" package, version 2.1.0). Piecewise structural equation modeling is a robust multivariate approach used to examine complex networks of relationships and uses Shipley's test of directed separation to evaluate if the specific pathway(s) should be excluded in an underspecified model [30]. Specifically, we fitted a full model including all potential pathways and then sequentially excluded nonsignificant pathways for the final model. For each component of the structural equation modeling, we conducted a linear mixed model with chamber treated as a random factor (the "*lme*" function; R "nlme" package, version 3.1–149). We evaluated the overall fit of the final model using Fisher's *C* statistic and the Akaike information criteria (*AIC*). We estimated the importance of each examined factor using its standardized total effect, which takes into account the direct and indirect effects of the factor on carbon fluxes.

We calculated the annual CO_2 and CH_4 budgets of the studied ecosystems by summing their gap-filled daily or hourly fluxes during the entire year. We divided the annual budget into different seasons (Table S2), which were delineated based on the 7-day moving average of soil temperature at 5-cm (ST_5) and 30-cm depths (ST_{30}) [17]. Specifically, the spring thaw was defined to start on the first of five consecutive days that the ST_5 exceeded –0.75 °C and to end on the day that the ST_{30} exceeded 0.75 °C. The autumn freeze was defined to start on the first of the five consecutive days that the ST_5 became lower than 0.75 °C and to end on the day that the ST_{30} started to be lower than –0.75 °C. The winter frozen was defined as the time between the end of autumn freeze in the previous year and the onset of spring thaw. The growing season was defined as the time between the end of spring thaw and the onset of autumn thaw. We used linear regression to examine the responses of the growing-season CO_2 and CH_4 budgets to interannual variability in temperature and precipitation.

We assessed the climate radiative forcing of the annual NEE and CH_4 budgets using the concept of the 100-year GWP, which has been adopted by the Intergovernmental Panel on Climate Change. The GWP methodology considers the atmospheric lifetime and radiative properties of greenhouse gasses and can evaluate the trade-offs between the climate impacts of CO_2 and CH_4 emissions by putting their time-integrated radiative impacts into CO_2 equivalents (CO_2-eq) [31]. The 100-year GWP (in g CO_2-eq m^{-2}) was calculated as follows [14]:

$$GWP = NEE \times 1 + CH_4 \times 28$$

where NEE is the annual NEE budget (in g CO_2 m^{-2}), and CH_4 is the annual CH_4 budget (in g CH_4 m^{-2}).

We conducted two-way analysis of variance to examine the effects of ecosystem type, sampling year and their interactions on the soil carbon pool, gaseous carbon budgets and GWP (Table S3). We further used Tukey's significant difference testing to test for the differences among ecosystems. In this study, all statistical analyses were conducted using R version 4.0.3 [32].

3. Results

3.1. Net ecosystem CO_2 exchange

The NEE of all three ecosystems followed a similar seasonal pattern with a net uptake period during the growing season (Figs. 2 and S3). However, the length of the net CO_2 uptake period in mesic meadow (148 days) was 1.9 and 1.6 times that in wet meadow and fen across the years 2012–2014, respectively. The mesic meadow had the highest peak CO_2 uptake rate, 97.8% higher than that of wet meadow and 5.6% higher than that of fen. The dominant predictors of the growing season NEE dynamic shifted from soil temperature in mesic meadow to soil temperature and water table in wet meadow, and then to water ta-

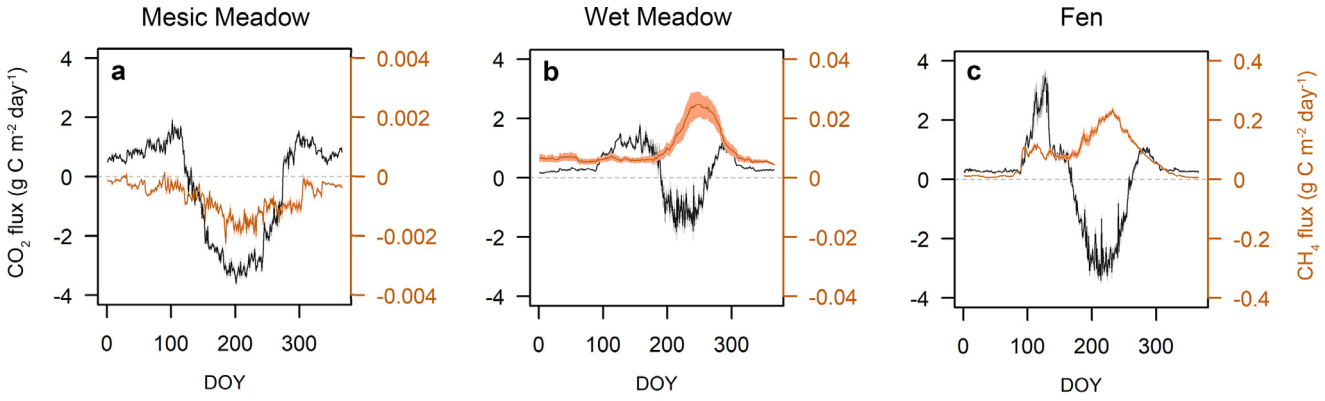

Fig. 2. Seasonal dynamics of net ecosystem CO_2 and CH_4 exchanges. (a) Mesic meadow; (b) wet meadow; (c) fen. Data are shown as the mean ± standard error (n = 5).

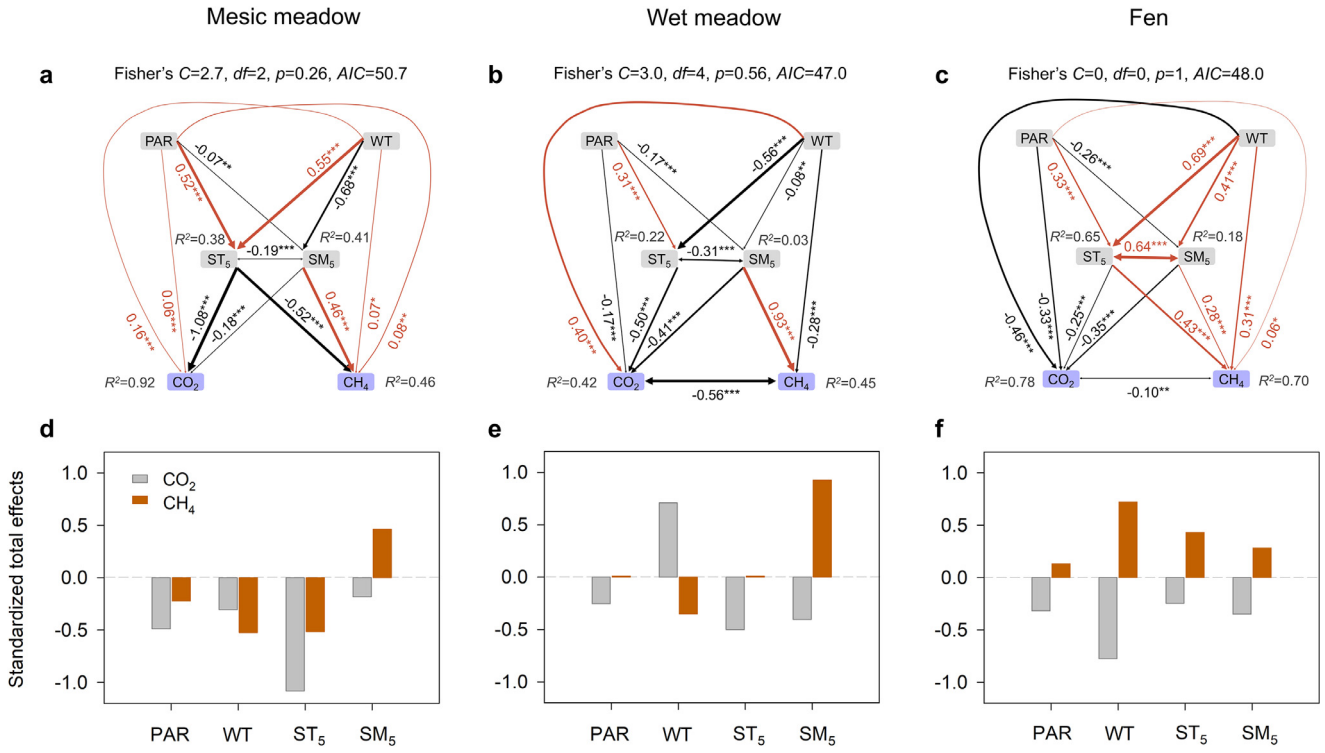

Fig. 3. Structural equation modeling examining effects of abiotic factors on net ecosystem CO_2 and CH_4 exchanges. (a–c) The networks of relationships between gaseous carbon fluxes and abiotic factors in the mesic meadow, wet meadow and fen; (d–f) the standardized total effects of abiotic factors for each ecosystem. The analyses are based on the monitoring data across the growing seasons from 2012 to 2014. The abiotic factors include photosynthetically active radiation (PAR), water table depth (WT), and soil temperature (ST_5) and moisture at 5 cm depth (SM_5). In (a-c), the solid red and black arrows represent significant positive and negative relationships, respectively; *, $p < 0.05$; **, $p < 0.01$; ***, $p < 0.001$. The arrow width is proportional to the strength of the relationship. The numbers near the arrows represent the standardized path coefficients. Marginal R^2 indicates the explained proportion of variance for each dependent variable in the models.

ble in fen (Figs. 3 and S6). In contrast, these ecosystems exhibited net CO_2 emissions during the nongrowing season. The mesic meadow had a larger CO_2 emission than the other two ecosystems in winter (Fig. 4a), while the fen produced a substantial pulse of CO_2 emission during spring thaw (Fig. 2).

The growing season NEE and its components (ER and GEP) gradually decreased along the succession gradient (Fig. S7). However, the annual NEE budget did not exhibit a gradient change across 2012–2014 and shifted from a carbon gain of 114.7 g C m^{-2} in mesic meadow to a carbon loss of 91.8 g C m^{-2} in wet meadow and then to carbon neutral in fen (Fig. 4a). The CO_2 emissions during the nongrowing season canceled out 56.7% of mesic meadow CO_2 uptake and 117.7% of fen CO_2 uptake during the growing season, and the nongrowing season CO_2 emissions dominated the annual NEE budget of the wet meadow. In addition, the CO_2 emissions during spring thaw increased gradually from mesic meadow to wet meadow and then to fen, which contributed to 38.2%, 61.4% and 67.8% of their corresponding nongrowing emissions, respectively (Figs. 4a and S8).

The growing season NEE of the three ecosystems showed different responses to interannual variations in air temperature and precipitation (Fig. S9). The mesic meadow exhibited an enhancement in net CO_2 uptake with increased growing season temperature from 2010 to 2014, while the wet meadow and fen did not exhibit any significant change with interannual temperature variations.

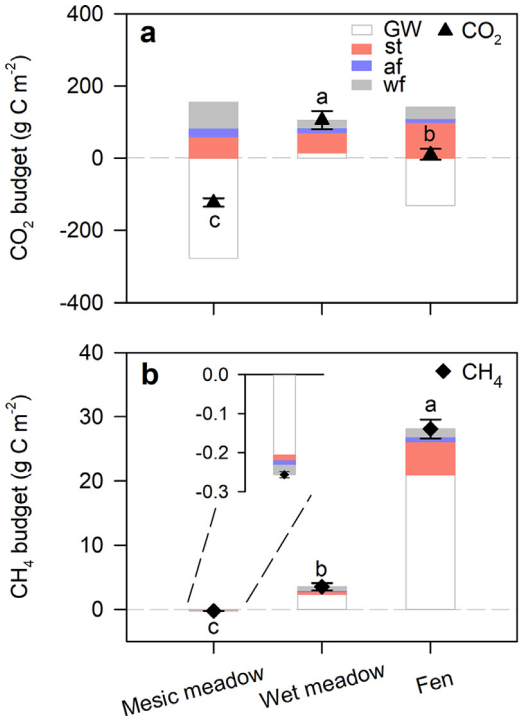

Fig. 4. Annual budget and seasonal distributions of net ecosystem CO_2 and CH_4 exchanges. (a) CO_2; (b) CH_4. The annual budget is the average value from 2012 to 2014, and we divided it into four different seasons, including the growing season (GW), spring thaw (st), autumn freeze (af) and winter frozen (wf). The bar shows the standard error of the mean ($n = 5$). The different letters above the bars indicate significant differences among ecosystems at $p < 0.05$ level.

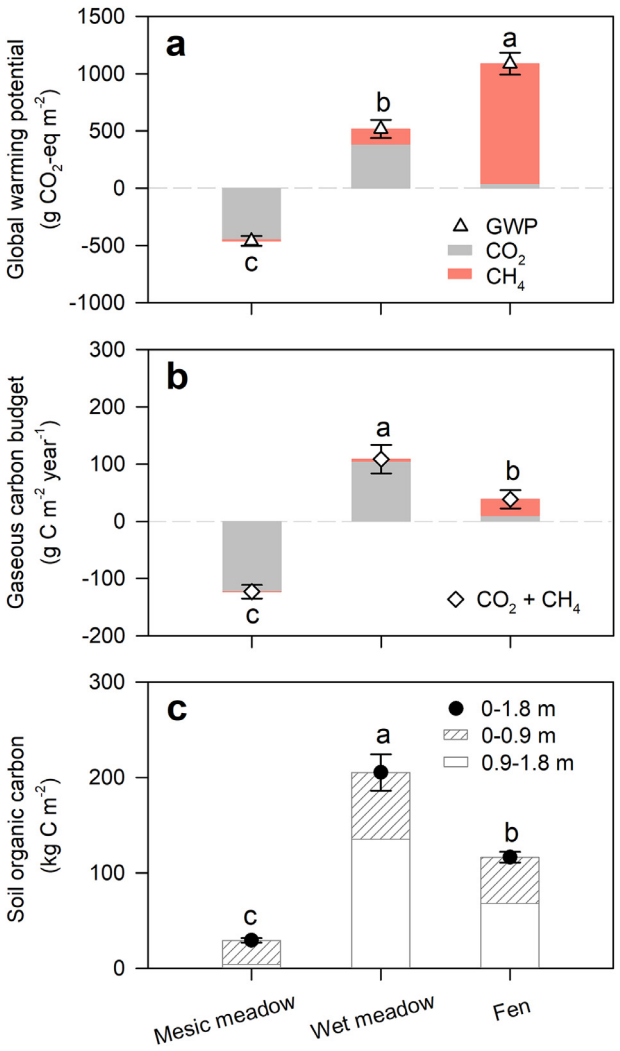

Fig. 5. Global warming potential, annual gaseous carbon budget and soil organic carbon density. (a) Global warming potential (GWP at 100-year time horizon); (b) annual carbon budget of net ecosystem CO_2 and CH_4 exchanges; (c) soil organic carbon density. The bar shows the standard error of the mean ($n = 5$ for GWP and gaseous carbon budget and $n = 3$ for soil organic carbon). The different letters above the bars indicate significant differences among ecosystems at $p < 0.05$ level.

3.2. Methane fluxes

The seasonal dynamics of CH_4 fluxes differed among ecosystems from 2012 to 2014 (Figs. 2 and S3). The mesic meadow absorbed CH_4 and reached the maximum rate around late July, the wet meadow released CH_4 and peaked in early September, and the fen showed two peak CH_4 emissions with a large peak in the middle of August and a small peak during spring thaw. The growing season CH_4 dynamics were regulated by soil temperature and soil moisture/water table depth in the mesic meadow and fen but dominated by soil moisture in the wet meadow (Figs. 3 and S6).

From 2012 to 2014, the annual CH_4 budget shifted from a sink of 0.3 g C m^{-2} for mesic meadow to a source of 3.5 g C m^{-2} for wet meadow and 28.0 g C m^{-2} for fen (Fig. 4b). The nongrowing season CH_4 exchanges accounted for 19.4–35.2% of the annual budgets in the studied ecosystems. Moreover, the nongrowing season CH_4 exchanges mainly occurred during the winter frozen in mesic meadow (48.8%) and wet meadow (43.9%) but were concentrated in the spring thaw in fen (71.9%) (Figs. 4b and S8).

The mesic meadow exhibited the largest growing season CH_4 uptake in the anomalously dry year (2012) of our study period, while the fen produced a stronger CH_4 emission in warmer years (2010 and 2013) (Fig. S9). The growing season CH_4 emission of wet meadow was not significantly affected by interannual variations in temperature and precipitation.

3.3. GWP of the annual NEE and CH_4 budgets and soil organic carbon stock

Based on the annual CO_2 and CH_4 budgets across 2012–2014, the 100-year GWP increased from –459.9 g CO_2-eq m^{-2} (cooling) in mesic meadow to 517.0 g CO_2-eq m^{-2} (warming) in wet meadow and then to 1087.4 g CO_2-eq m^{-2} in fen (Fig. 5a). Moreover, the enhancement in the GWP during paludification was largely due to the increased CH_4 emissions.

The annual gaseous carbon budget was –123.1 g C m^{-2} (sink) for mesic meadow, 108.8 g C m^{-2} (source) for wet meadow and 38.7 g C m^{-2} for fen across 2012–2014 (Fig. 5b), suggesting that paludification may cause gaseous carbon loss. In contrast, the 0–1.8 m soil survey showed 7.0- and 4.0-fold larger soil organic carbon in the wet meadow and fen than in the mesic meadow, respectively (Fig. 5c), indicating that paludification produced an accumulation of soil carbon.

4. Discussion

Our findings did not support the first hypothesis and showed that paludification reduced the net ecosystem CO_2 uptake in addition to increasing the CH_4 emissions. Paludification also altered the temporal dynamics of the CO_2 and CH_4 fluxes, which were regulated by changes in dominant abiotic predictors and spring-thaw emissions. In contrast, our

results showed that paludification produced a large accumulation of soil organic carbon and a higher GWP, which supported the second hypothesis. However, the soil organic carbon accumulation was in contrast with a shift from gaseous carbon uptake to release, suggesting a potential role of nongaseous carbon pathways in regulating the soil carbon budget during paludification. These findings will deepen our understanding of the development of the carbon cycle during alpine biogeomorphic succession and improve the long-term assessment of the wetland carbon footprints under climate change.

4.1. Shifts in the patterns and drivers of CO_2 flux during succession

Our result of the gradual reductions in GPP and ER during paludification was likely associated with the reduced soil aeration, which slowed the mineralization of nutrients for plant growth and the decomposition of organic matter [9,10]. We further found that paludification turned the ecosystem from a net sink of CO_2 to a net source and then to a neutral source. This result reflected that the developments of GPP and ER were not synchronous in magnitude. The reduction in GPP outpaced that in ER when mesic meadow developed to wet meadow, which was likely because the dominant species *Kobresia tibetica* in wet meadow has a low photosynthetic capacity and a short growing season [33]. In contrast, as wet meadow further developed to fen, ER exhibited a larger reduction than GPP. This may be largely associated with the flooding of the topsoil layer in fen, and respiration from topsoil often dominates total soil respiration [34].

We found that the dominant predictors of growing season NEE dynamics shifted from soil temperature alone to soil temperature and water table, and then to water table during paludification. This finding supported a past study reporting that temperatures dominate NEE in alpine mesic meadows [35]. This result may be because low temperatures constrained the activity of plants and soil microbes at our high-elevation site with large temperature variation (~15.0 ˚C at a 5 cm soil depth during June-October) (Fig S2a). However, water table depth overrode soil temperature in regulating NEE dynamics in fen, which may have been because waterlogged conditions reduced seasonal variation in soil temperature (~13.6 ˚C) due to the high specific heat capacity of water. Meanwhile, it may be related to the fact that the water table depth regulated the seasonality of soil respiration in the fen [12].

Our results showed that the nongrowing season CO_2 emissions largely offset or even exceeded the CO_2 uptakes during the growing seasons, suggesting a vital contribution of nongrowing season emissions to the annual CO_2 budget. We further found that succession changed the key period of CO_2 emissions during nongrowing seasons. In the present study, high winter CO_2 emissions occurred in mesic meadows, which may have been due to daytime CO_2 emissions during the diurnal freezing and thawing cycle of surface soil [27]. In contrast, the nongrowing season CO_2 emissions did not occur in winter frozen but were concentrated in spring thaw in the fen. This was likely because the thick ice cover of fen in winter hindered soil CO_2 diffusivity and reduced microbial CO_2 production by inhibiting the diffusion of atmospheric oxygen into soils [36]. As the ice melted in spring, the rising temperature, the increasing water and nutrient availability and the activated microbes together might accelerate the decomposition of soil organic matter and plant litter and cause substantial CO_2 emissions [37–39]. Overall, these findings suggested that alpine succession caused a shift in the key period of CO_2 emissions during the nongrowing season, largely due to the changes in the soil freeze-thaw process.

4.2. Shifts in the patterns and drivers of CH_4 fluxes during succession

We found that the ecosystem shifted from a weak sink of CH_4 to a strong source of CH_4 as paludification proceeded. The studied mesic meadow absorbed 0.3 g C m^{-2} $year^{-1}$ of CH_4, which was within the range of 0.062–0.48 g C m^{-2} $year^{-1}$ from other reports in Tibetan alpine grasslands [40,41]. In contrast, the annual CH_4 emissions in the studied wet meadow and fen were one and two orders of magnitude higher than the annual CH_4 uptake in the mesic meadow, respectively. The CH_4 emissions of wet meadow (3.5 g C m^{-2}) were comparable to those observed in Arctic tundra and boreal bogs [42], while the fen CH_4 emissions (28.0 g C m^{-2}) were within the upper range of emissions from boreal peatlands [42] but lower than the emissions from temperate coastal marsh (50.8 g C m^{-2}) [43]. In this study, the observed change in CH_4 flux during paludification may be due to the enhanced CH_4 production associated with the increase in soil methanogens, as well as the decreasing CH_4 oxidation related to the increase in sedge plants with well-developed aerenchyma that transported CH_4 to the atmosphere bypassing the soil oxidized zone (Table S1).

Our analysis showed that the dominant predictors of seasonal CH_4 flux dynamics varied with succession. Soil temperature and soil moisture/water table depth together controlled the CH_4 fluxes at the mesic meadow and the fen, suggesting a synergistic effect of temperature and water. This finding is in line with a previous study in high-latitude permafrost zones reporting that CH_4 emissions were more sensitive to soil temperature in wetter ecosystems but more sensitive to water table in drier ecosystems [44]. However, we found that soil moisture, but not soil temperature, dominated the dynamics of CH_4 emissions in the wet meadow. This may result from counteracting temperature effects on the activity of soil methanogens and methanotrophs, which are highly temperature-sensitive [6,41].

We revealed that the key period of CH_4 fluxes differed at different stages of paludification. The mesic meadow absorbed CH_4 in the long frozen period, likely because the diurnal freeze-thaw process in surface soil favored soil methanotrophs by increasing temperature and water availability. It has been reported that cold temperature and low water availability in soil pores may inhibit soil methanotroph activity in Tibetan alpine grasslands [40,41]. In contrast, the CH_4 emissions in our studied fen were concentrated during the spring thaw period. This was likely associated with the thick ice cover and the permanent active soil layer approximately 1 m below the soil surface [45]. The ice cover was completed during late fall and inhibited CH_4 oxidation in the surface soil by isolating the soil from atmospheric oxygen, whereas the permanent active layer favored the production and accumulation of CH_4 in deep soil [17]. The accumulated CH_4 in soils was rapidly released when the ice and frozen topsoil melted during spring [18].

4.3. Paradox between the changes in gaseous carbon flux and soil carbon pool during succession

A crucial finding in our study is the seeming paradox between gaseous carbon loss and soil carbon accumulation during paludification. One potential explanation is that the nongaseous ecosystem carbon exchange contributed to soil carbon accumulation. For example, lateral carbon transport in the form of dissolved or/and particulate carbon could contribute substantially to the carbon budget of peatland ecosystems in northern high-latitude regions [46–48]. In this study, the low-lying wet meadow and fen could receive carbon in runoff from the surrounding mesic meadows during heavy rain events [48]. The fen may also receive carbon from groundwater. The lateral carbon input may offset the gaseous loss of carbon from these wetlands and lead to soil carbon accumulation over a long time.

Another possible explanation for the observed paradox is the mismatch in the time scale of the observed gaseous carbon loss and soil carbon accumulation [48,49]. While net gaseous carbon loss was observed over the three years studied, the soil carbon pools of these wetlands were the result of carbon sequestration over centuries to millennia [50]. Our observed gaseous flux over the three years may not represent the historical pattern of carbon flux in these wetlands. Alternatively, the length of the study may not be long enough to fully capture the temporal variability in carbon flux in these systems. For example, the net gaseous carbon budget of fen changed from a source of 38.7 g C m^{-2} yr^{-1} to a

sink of 21.7 g C m^{-2} yr^{-1} if we excluded data from the dry year 2012. Thus, the observed gaseous carbon loss does not necessarily contradict the increased soil carbon accumulation along the paludification gradient.

We observed an increasing GWP along the stages of paludification, driven primarily by increasing CH_4 emissions. This finding is consistent with our previous water table manipulation experiment in the same wetland [9]. However, we cannot simply interpret the higher GWP as a warming impact on the climate system, and whether paludification produces a warming or cooling climate impact depends on the source of the carbon accumulated in the soil. If the observed increasing GWP in this study is only temporary while the soil carbon accumulation results from the net gaseous carbon uptake historically, paludification should exert an overall cooling impact on the climate system [42]. In contrast, if the increasing GWP is long-lasting and such soil carbon accumulation represents a translocation of carbon from nearby mesic meadows, paludification would accelerate climate warming.

Over the past decades, climate warming has led to accelerated glacier and permafrost melting, an expanded wetland area, and a higher lateral carbon input into wetlands on the Tibetan Plateau [51,52]. Understanding the contribution of lateral carbon transport is crucial for characterizing both the carbon budget of alpine ecosystems that are connected hydrologically and the carbon footprint of alpine wetlands during biogeomorphic succession. We therefore suggest that a catchment-scale monitoring network of lateral carbon flows on the Tibetan Plateau is urgently established. Future research should pay more attention to the pattern and drivers of lateral carbon flows and elucidate the fate of carbon (respiratory CO_2, carbon deposits, or carbon transfer) during lateral transport [52,53].

5. Conclusion

In summary, this study showed that the alpine biogeomorphic succession towards wetlands prompted a CH_4-dominated increase in gaseous carbon emissions in concurrence with soil carbon accumulation. The findings have several important implications. First, this work provides comprehensive gaseous carbon flux monitoring at different stages of alpine wetland succession, and the dataset can be used to benchmark and parameterize Earth system models to produce credible projections of carbon emissions for alpine ecosystems. Second, our results suggest that the carbon flux dynamics during succession are driven by shifts in the biotic community, changes in the dominant abiotic drivers and soil freeze-thaw process, which should be incorporated into next-generation models. Finally, the paradox between the contemporary gaseous carbon budget and the soil organic pool change suggests a potential contribution of the lateral carbon exchange and/or changing climates to long-term climate-carbon feedback during alpine biomorphic succession.

Declaration of competing interest

The authors declare that they have no conflicts of interest in this work.

CRediT authorship contribution statement

Hao Wang: Investigation, Conceptualization, Writing – original draft, Writing – review & editing. **Lingfei Yu:** Investigation, Writing – review & editing. **Litong Chen:** Investigation, Writing – review & editing. **Zhenhua Zhang:** Investigation, Writing – review & editing. **Xuefei Li:** Writing – review & editing. **Naishen Liang:** Investigation, Writing – review & editing. **Changhui Peng:** Writing – review & editing. **Jin-Sheng He:** Visualization, Conceptualization, Investigation, Writing – review & editing.

Acknowledgments

We thank Weimin Song, Zhaorong Mi, Chao Wang and Guangshuai Wang for collecting the field data and Zhenong Jin, Chao Song, Shushi Peng and Yahai Lu for their insightful suggestions on an earlier conception of this manuscript. This study was supported by the National Natural Science Foundation of China (32130065, 31901145, 32111530062), the Discipline Construction Fund of Peking University and the Academy of Finland (341294).

Supplementary materials

Supplementary material associated with this article can be found, in the online version, at doi:10.1016/j.fmre.2022.09.024.

References

[1] W.J. Mitsch, B. Bernal, A.M. Nahlik, et al., Wetlands, carbon, and climate change, Landscape Ecol. 28 (2013) 583–597.
[2] M. Saunois, A.R. Stavert, B. Poulter, et al., The Global Methane Budget 2000–2017, Earth Syst. Sci. Data 12 (2020) 1561–1623.
[3] N.C. Davidson, E. Fluet-Chouinard, C.M. Finlayson, Global extent and distribution of wetlands: trends and issues, Mar. Freshwater Res. 69 (2018) 620–627.
[4] R.J.M. Temmink, L.P.M. Lamers, C. Angelini, et al., Recovering wetland biogeomorphic feedbacks to restore the world's biotic carbon hotspots, Science 376 (2022) eabn1479.
[5] J. Eichel, Vegetation succession and biogeomorphic interactions in glacier forelands, in: Geomorphology of Proglacial Systems, Springer, Cham, 2019, pp. 327–349.
[6] J.L. Bubier, T.R. Moore, An ecological perspective on methane emissions from northern wetlands, Trends Ecol. Evol. 9 (1994) 460–464.
[7] C.K. McCalley, B.J. Woodcroft, S.B. Hodgkins, et al., Methane dynamics regulated by microbial community response to permafrost thaw, Nature 514 (2014) 478–481.
[8] J.F. Pekel, A. Cottam, N. Gorelick, et al., High-resolution mapping of global surface water and its long-term changes, Nature 540 (2016) 418–422.
[9] H. Wang, L. Yu, Z. Zhang, et al., Molecular mechanisms of water table lowering and nitrogen deposition in affecting greenhouse gas emissions from a Tibetan alpine wetland, Glob. Change Biol. 23 (2017) 815–829.
[10] S.L. Malone, G. Starr, C.L. Staudhammer, et al., Effects of simulated drought on the carbon balance of Everglades short-hydroperiod marsh, Glob. Change Biol. 19 (2013) 2511–2523.
[11] H. Joosten, D. Clarke, Wise use of mires and peatlands-background and principles including a framework for decisionmaking, Int. Mire Conserv. Group Int. Peat Soc. (2002).
[12] L. Yu, H. Wang, Y. Wang, et al., Temporal variation in soil respiration and its sensitivity to temperature along a hydrological gradient in an alpine wetland of the Tibetan Plateau, Agric. Forest Meteorol. (2020) 282–283.
[13] D. Olefeldt, E.S. Euskirchen, J. Harden, et al., A decade of boreal rich fen greenhouse gas fluxes in response to natural and experimental water table variability, Glob. Change Biol. 23 (2017) 2428–2440.
[14] IPCC, Climate change 2013: the physical science basisProceedings of the Contribution of Working Group I to the Fifth Assessment Report of the Intergovernmental Panel on Climate Change, Cambridge University Press, 2013.
[15] H.F. Jungkunst, S. Fiedler, Latitudinal differentiated water table control of carbon dioxide, methane and nitrous oxide fluxes from hydromorphic soils: feedbacks to climate change, Glob. Change Biol. 13 (2007) 2668–2683.
[16] M. Mastepanov, C. Sigsgarrd, E.J. Dlugokencky, et al., Large tundra methane burst during onset of freezing, Nature 456 (2008) 628–630.
[17] D. Zona, B. Gioli, R. Commane, et al., Cold season emissions dominate the Arctic tundra methane budget, Proc. Natl. Acad. Sci. U. S. A. 113 (2016) 40–45.
[18] W.M. Song, H. Wang, G. Wang, et al., Methane emissions from an alpine wetland on the Tibetan Plateau: neglected but vital contribution of the nongrowing season, J. Geophys. Res. Biogeosci. 120 (2015) 1475–1490.
[19] J. Xu, R.E. Grumbine, A. Shrestha, et al., The melting Himalayas: cascading effects of climate change on water, biodiversity and livelihoods, Conserv. Biol. 23 (2009) 520–530.
[20] J. Ding, F. Li, G. Yang, et al., The permafrost carbon inventory on the Tibetan Plateau: a new evaluation using deep sediment cores, Glob. Change Biol. 22 (2016) 2688–2701.
[21] H. Chen, Q. Zhu, C. Peng, et al., The impacts of climate change and human activities on biogeochemical cycles on the Qinghai-Tibetan Plateau, Glob. Change Biol. 19 (2013) 2940–2955.
[22] G. Zhang, H. Xie, S. Kang, et al., Monitoring lake level changes on the Tibetan Plateau using ICESat altimetry data (2003–2009), Remote Sens. Environ. 115 (2011) 1733–1742.
[23] G. Cheng, T. Wu, Responses of permafrost to climate change and their environmental significance, Qinghai-Tibet Plateau, J. Geophys Res. 112 (2007) F02S03.
[24] Z. Xue, Z. Zhang, X. Lu, et al., Predicted areas of potential distributions of alpine wetlands under different scenarios in the Qinghai-Tibetan Plateau, China, Glob. Planet. Change 123 (2014) 77–85.
[25] M. Ma, X. Zhou, G. Du, Soil seed bank dynamics in alpine wetland succession on the Tibetan Plateau, Plant Soil 346 (2011) 19–28.

[26] G.H. Ren, B. Deng, Z.H. Shang, et al., Plant communities and soil variations along a successional gradient in an alpine wetland on the Qinghai-Tibetan Plateau, Ecol. Eng. 61 (2013) 110–116.
[27] Y.H. Wang, H. Liu, H. Chung, et al., Non-growing-season soil respiration is controlled by freezing and thawing processes in the summer monsoon-dominated Tibetan alpine grassland, Glob. Biogeochem. Cycles 28 (2014) 1081–1095.
[28] S. Dengel, D. Zona, T. Sachs, et al., Testing the applicability of neural networks as a gap-filling method using CH_4 flux data from high latitude wetlands, Biogeosciences 10 (2013) 8185–8200.
[29] D. Papale, R. Valentini, A new assessment of European forests carbon exchanges by eddy fluxes and artificial neural network spatialization, Glob. Change Biol. 9 (2003) 525–535.
[30] J.S. Lefcheck, S.E.M. Piecewise, Piecewise structural equation modelling in R for ecology, evolution, and systematics, Methods Ecol. Evol. 7 (2016) 573–579.
[31] S. Frolking, N. Roulet, J. Fuglestvedt, How northern peatlands influence the Earth's radiative budget: sustained methane emission versus sustained carbon sequestration, J. Geophys. Res. 111 (2006) G01008.
[32] R.C. TeamR: A language and Environment For Statistical Computing, R Foundation for Statistical Computing, Vienna, Austria, 2018.
[33] J.S. He, Z. Wang, X. Wang, et al., A test of the generality of leaf trait relationships on the Tibetan Plateau, New Phytol 170 (2006) 835–848.
[34] H. Wang, L.F. Yu, L.T. Chen, et al., Responses of soil respiration to reduced water table and nitrogen addition in an alpine wetland on the Qinghai-Xizang Plateau, Chin. J. Plant Ecol. 38 (2014) 619–625 in Chinese with an English abstract.
[35] M. Saito, T. Kato, Y.H. Tang, Temperature controls ecosystem CO_2 exchange of an alpine meadow on the northeastern Tibetan Plateau, Glob. Change Biol. 15 (2009) 221–228.
[36] M.A. Mast, K.P. Wickland, R.T. Striegl, et al., Winter fluxes of CO_2 and CH_4 from subalpine soils in rocky mountain national park, Colorado, Glob. Biogeochem. Cycles 12 (1998) 607–620.
[37] J.S. Clein, J.P. Schimel, Microbial activity of tundra and taiga soils at sub-zero temperatures, Soil Biol. Biochem. 27 (1995) 1231–1234.
[38] D.G. Kim, R. Vargas, B. Bond-Lamberty, et al., Effects of soil rewetting and thawing on soil gas fluxes: a review of current literature and suggestions for future research, Biogeosciences 9 (2012) 2459–2483.
[39] W.C. Oechel, G. Vourlitis, S.J. Hastings, Cold season CO_2 emission from arctic soils, Glob. Biogeochem. Cycles 11 (1997) 163–172.
[40] Z. Zhang, G. Wang, H. Wang, et al., Warming and drought increase but wetness reduces the net sink of CH_4 in alpine meadow on the Tibetan Plateau, Appl. Soil Ecol. 167 (2021) 104061.
[41] P. Wang, J. Wang, B. Elberling, et al., Increased annual methane uptake driven by warmer winters in an alpine meadow, Glob. Change Biol. 28 (2022) 3246–3259.
[42] A.M. Petrescu, A. Lohila, J.P. Tuovinen, et al., The uncertain climate footprint of wetlands under human pressure, Proc. Natl. Acad. Sci. U. S. A. 112 (2015) 4594–4599.
[43] H. Chu, J.F. Gottgens, J. Chen, et al., Climatic variability, hydrologic anomaly, and methane emission can turn productive freshwater marshes into net carbon sources, Glob. Change Biol. 21 (2015) 1165–1181.
[44] D. Olefeldt, M.R. Turetsky, P.M. Crill, et al., Environmental and physical controls on northern terrestrial methane emissions across permafrost zones, Glob. Change Biol. 19 (2013) 589–603.
[45] Y.N. Li, X.K. Bao, G.M. Cao, Observation of soil temperature regime in cryic-wetland at the depth of 40–80cm at Haibei, Qilian mountains, J. Glaciol. Geocryol. 22 (2000) 153–158 in Chinese with an English abstract.
[46] N.T. Roulet, P.M. Lafleur, P.J.H. Richard, et al., Contemporary carbon balance and late Holocene carbon accumulation in a northern peatland, Glob. Change Biol. 13 (2007) 397–411.
[47] M. Nilsson, J. Sagerfors, I. Buffam, et al., Contemporary carbon accumulation in a boreal oligotrophic minerogenic mire-a significant sink after accounting for all C-fluxes, Glob. Change Biol. 14 (2008) 2317–2332.
[48] A.K. Koehler, M. Sottocornola, G. Kiely, How strong is the current carbon sequestration of an Atlantic blanket bog? Glob. Change Biol. 17 (2011) 309–319.
[49] W.C. Oechel, S.J. Hastings, G. Vourlrtis, et al., Recent change of Arctic tundra ecosystems from a net carbon dioxide sink to a source, Nature 361 (1993) 520–523.
[50] N.B. Dise, Peatland response to global change, Science 326 (2009) 810–811.
[51] C. Song, G. Wang, Land carbon sink of the Tibetan Plateau may be overestimated without accounting for the aquatic carbon export, Proc. Natl. Acad. Sci. U. S. A. 118 (2021) e2114694118.
[52] L. Ran, D.E. Butman, T.J. Battin, et al., Substantial decrease in CO_2 emissions Chinese inland waters due to global change, Nat. Commun. 12 (2021) 1730.
[53] P. Regnier, L. Resplandy, R.G. Najjar, et al., The land-to-ocean loops of the global carbon cycle, Nature 603 (2022) 401–410.

Hao Wang is a young researcher at the State Key Laboratory of Herbage Improvement and Grassland Agro-ecosystems, and the College of Ecology, Lanzhou University, China. His-research focuses on how climate change influences the carbon cycle of alpine ecosystems on the Tibetan Plateau, including plant growth, greenhouse gas emissions and soil organic carbon dynamics.

Jin-Sheng He is a professor at the State Key Laboratory of Herbage Improvement and Grassland Agro-ecosystems, Lanzhou University, and the Institute of Ecology, Peking University, China. His-research focuses on how global changes affect the alpine grassland ecosystems on the Tibetan Plateau and has centered on these areas including above- and belowground biodiversity and ecosystem functioning, connections among soil organisms, herbivores, plants, and ecosystem function, and scale-dependent interactions of shifting ecosystem composition, phenology, and ecological processes.